Magnetoencephalographic Gamma Power Reduction in Patients with Schizophrenia During Resting Condition

Lindsay Rutter,[1] Frederick W. Carver,[1] Tom Holroyd,[1]
Sreenivasan Rajamoni Nadar,[1] Judy Mitchell-Francis,[1] Jose Apud,[2]
Daniel R. Weinberger,[2] and Richard Coppola[1,2]*

[1]*MEG Core Facility, National Institute of Mental Health, Bethesda, Maryland*
[2]*Clinical Brain Disorders Branch, NIMH, Bethesda, Maryland*

◆ ═══════════════════════════════════ ◆

Abstract: *Objective:* The "default network" represents a baseline condition of brain function and is of interest in schizophrenia research because its component brain regions are believed to be aberrant in the disorder. We hypothesized that magnetoencephalographic (MEG) source localization analysis would reveal abnormal resting activity within particular frequency bands in schizophrenia. *Experimental Design:* Eyes-closed resting state MEG signals were collected for two comparison groups. Patients with schizophrenia ($N = 38$) were age-gender matched with healthy control subjects ($N = 38$), and with a group of unmedicated unaffected siblings of patients with schizophrenia ($N = 38$). To localize 3D-brain regional differences, synthetic aperture magnetometry was calculated across established frequency bands as follows: delta (0.9–4 Hz), theta (4–8 Hz), alpha (8–14 Hz), beta (14–30 Hz), gamma (30–80 Hz), and super-gamma (80–150 Hz). *Principle Observations:* Patients with schizophrenia showed significantly reduced activation in the gamma frequency band in the posterior region of the medial parietal cortex. As a group, unaffected siblings of schizophrenia patients also showed significantly reduced activation in the gamma bandwidth across similar brain regions. Moreover, using the significant region for the patients and examining the gamma band power gave an odds ratio of 6:1 for reductions of two standard deviations from the mean. This suggests that the measure might be the basis of an intermediate phenotype. *Conclusions:* MEG resting state analysis adds to the evidence that schizophrenic patients experience this condition very differently than healthy controls. Whether this baseline difference relates to network abnormalities remains to be seen. *Hum Brain Mapp 30:3254–3264, 2009.* © 2009 Wiley-Liss, Inc.

Key words: default network; synthetic aperture magnetometry; baseline; precuneus; cuneus; SAM; magnetoencephalography; unaffected siblings; default mode

◆ ═══════════════════════════════════ ◆

INTRODUCTION

PET and fMRI brain imaging studies in healthy humans have consistently revealed brain regions that are characterized by decreased activity during engagement in cognitively demanding tasks [Gusnard et al., 2001; McKiernan et al., 2003; Raichle et al., 2001; Shulman et al., 1997]. Furthermore, these brain areas are also reported to be the most metabolically active regions during task-independent, resting state studies [Gusnard and Raichle, 2001]. Such

observations have led Raichle et al. [Raichle et al., 2001] to propose an organized "default mode" network of the brain that is active during rest and attenuated during cognitive tasks. The exact purpose and significance of the spontaneous mental processing that occurs during rest is unknown. However, it is suggested that when an individual is awake and alert but not actively participating in goal-directed activity, brain regions, like the precuneus as well as the posterior cingulate cortex (PCC) and medial prefrontal cortices (mPFC), perform ongoing information processing and representation of the self and the external world [Gusnard and Raichle, 2001].

Interestingly, task-induced deactivation (TID) of the default network appears to increase with increasing task difficulty and working memory load [Esposito et al., 2006; McKiernan et al., 2003]. Furthermore, in situations where the shift from a self-focused resting state to an externally-focused cognitive state is less effective (i.e., slower reaction times), less midline TID is observed [Lawrence et al., 2003; Weissman et al., 2006]. These trends are consistent with the hypothesis that the default mode is involved in continuous information gathering; in situations that require cognitive attention, fewer resources can be allocated to this broad, self-referential baseline activity [Greicius and Menon, 2004].

There is evidence to suggest that patients with schizophrenia may show an atypical functional profile within the so-called default network; in addition to being implicated in attending to external and internal stimuli, the default network is also postulated to represent reflective activity that includes episodic memory retrieval, inner speech, and mental images [Greicius and Menon, 2004; Mazoyer et al., 2001]. These neural mechanisms are hypothesized to be anomalous in schizophrenia. For instance, Frith [Frith, 1995] has argued that a predilection to attribute internally generated thought (inner speech) as arising endogenously is fundamental to the disorder. Similarly, schizophrenic patients are well-known to display clear deficits in episodic memory retrieval measures [Goldberg et al., 2003].

A recent fMRI study investigating the nature of TIDs in schizophrenic patients found that patients displayed greater mPFC TIDs when compared with healthy control subjects [Harrison et al., 2007]. The authors concluded that the more pronounced TIDs reflect a greater experience of task demand in schizophrenic patients, consistent with extensive reports of cognitive inefficiency in schizophrenia. Additionally, patients who demonstrated poorer task performance showed a smaller TID effect, which was attributed to attentional lapses or interruption of cognitive processes with self-directed thoughts.

It is important to note that perturbation of activity in the default network can be achieved either by using demanding cognitive tasks or simple sensorimotor and resting state methods [Greicius and Menon, 2004; Greicius et al., 2003, 2004]. Cognitive tasks have the advantage that behavioral results may serve to confirm that subjects correctly performed the tasks; such monitoring is not available in resting states. However, the use of resting state designs is appealing because of the simplicity of the experimental setup. This is especially true for examining cognitively impaired patients because of the inherent difficulty of matching cognitive performance scores in healthy controls and patients before group-level statistical analysis [Esposito et al., 2006].

Recently, three separate fMRI laboratories have used resting state and simple sensorimotor designs to characterize default mode functional differences between schizophrenic patients and healthy controls [Bluhm et al., 2007; Garrity et al., 2007; Liang et al., 2006; Liu et al., 2008; Zhou et al., 2007a,b]. Garrity et al. [Garrity et al., 2007] used a simple auditory oddball task, along with independent component analysis (ICA), to extract default brain modes. Healthy controls demonstrated greater default mode activity than schizophrenic patients predominantly in the right PCC and bilateral precuneus and cingulate gyrus in low frequency oscillations (0.03 Hz) of the blood oxygen level-dependent (BOLD) signal. In contrast, schizophrenic patients showed increased default mode activity in the left PCC and bilateral anterior cingulate and superior and medial frontal gyri. The authors speculated that the laterality differences patients showed in various brain regions may suggest that the connectivity of the default mode network is altered in schizophrenia.

Similarly, Bluhm et al. [Bluhm et al., 2007] used an eyes-closed resting state design and correlated spontaneous low-frequency ($<$0.1 Hz) fluctuations of the BOLD signal between PCC and other brain regions. They reported less correlation between the PCC and the mPFC, lateral parietal, and cerebellar regions in schizophrenic patients than in healthy controls.

The third group performed four resting-state fMRI studies comparing healthy controls and schizophrenic patients that revealed baseline abnormalities in patients [Liang et al., 2006; Liu et al., 2008; Zhou et al., 2007a,b]. Two of their studies did not use predefined seed ROIs: They found whole-brain decreased functional connectivity in resting schizophrenia after computing the connectivities of all pairwise combinations of voxels throughout the entire brain [Liang et al., 2006], and they also found that schizophrenic patients demonstrated significantly altered small-world topological properties in several brain regions across the prefrontal, parietal, and temporal lobes [Liu et al., 2008]. The authors suggested that their resting findings "may partially account for the reduced global/local efficiency of information processing within the brain, which may lead to the deficits of cognition and behavior of patients with schizophrenia" [Liu et al., 2008].

It is worth emphasizing that all three fMRI groups found apparent anomalies of default network activity and connectivity in patients when compared with healthy controls in several brain areas as per slow frequency fluctuations of the BOLD signal. Liang et al. [Liang et al., 2006] cited one source to state that "low-frequency ($<$1 Hz) fluctuations from resting-state fMRI data are considered to be

physiologically meaningful and related to neural spontaneous activity." Moreover, Bluhm et al. [Bluhm et al., 2007] cited two sources in their speculation that the observed slow fluctuations of the BOLD signal may be associated with gamma fluctuations in electrophysiological signals [Bruns et al., 2000; Buzsaki and Draguhn, 2004].

Conversely, studies that assessed the electroencephalographic (EEG) signature of default mode activity in healthy controls demonstrated that beta power increased in the medial parietal regions during rest [Laufs et al., 2003]. As a result, we hypothesized that schizophrenic patients would display significantly different baseline activity when compared with healthy controls in specific magnetoencephalographic (MEG) frequency bands.

It should be noted that recent resting state studies have used MEG as a means to analyze clinical populations, including Alzheimer's disease [Stam et al., 2006], Parkinson's disease [Bosboom et al., 2006], and also schizophrenia as well as other disorders [Georgopoulos et al., 2007]. However, these studies examined cross correlations between MEG channels in sensor space, and thus do not allow interpretation in terms of localization of underlying activity. Source localization techniques allow us to estimate the anatomical source of neuromagnetic activity from the sensors located outside of the head.

To the best of our knowledge, this is the first study to examine healthy controls and schizophrenic patients in resting conditions using MEG source localization analysis. Consequently, we investigated several original questions: (1) Is MEG minimum variance source analysis suitable to detect the default network that is observed in other neuroimaging techniques? (2) If the default mode is identified, what neuromagnetic frequencies, if not gamma, are associated with the default network? (3) Is there a significant difference in the default network activity profile between medicated schizophrenic patients and healthy controls?

The concern remains, as in most clinical resting state studies, that our patients were all on antipsychotic medications during data collection. However, studying unaffected siblings of schizophrenic individuals will allow investigation of our measures as an "intermediate phenotype" without the conflict of medication [Callicott et al., 1998; Egan et al., 2000; Winterer et al., 2003].

We thus performed identical analyses between two comparison groups. The main comparison involved 38 healthy controls and 38 mostly medicated schizophrenic patients, and the second comparison involved 38 healthy controls and 38 nonmedicated, unaffected siblings of schizophrenic patients. Not all 38 unaffected siblings were directly related to a patient also used in this analysis because of the inherent difficulty of obtaining usable data from both persons of the same family. However, 10 schizophrenic patients had one unaffected sibling whose data was used, two patients had two unaffected siblings, and one patient had four unaffected siblings. Restated, although each unaffected sibling in this study was a direct sibling of a schizophrenic individual, only eighteen of the 38 unaffected siblings used in this analysis were siblings of schizophrenic patients also used in this analysis.

Similarly, to maintain an appropriate age-gender match for both comparison groups, the 38 healthy controls used in the main comparison (patients versus healthy controls) were completely separate from the 38 healthy controls used in the second comparison (unaffected siblings versus healthy controls) (see Materials and Methods). Our use of nonoverlapping control groups precluded the performance of a single comparison (ANOVA) across the three population groups.

MATERIALS AND METHODS

Subjects

Data collection occurred as part of the Clinical Brain Disorders Branch/National Institute of Mental Health Genetic Study of Schizophrenia (National Institutes of Health Study ID NCT00001486). Initial screening required that applicants had to be aged between 18 and 60 years, have a premorbid IQ score greater than 70, and be able to give informed consent. Applicants were disqualified if they had alcohol or drug abuse in the past 6 months, dependence in the past year, or more than a 5 year history of abuse or dependence. Healthy subjects were recruited from the community and through the National Institutes of Health (NIH) Normal Volunteer Office and were screened with an additional criterion that they did not have a first-degree relative with schizophrenia. Schizophrenic outpatients and their siblings were recruited from local and national sources. All procedures were approved by the National Institute of Mental Health (NIMH) Institutional Review Board. For more details on participant recruitment, evaluation, and potential ascertainment biases, see Egan et al. [Egan et al., 2000]. In the current study, all subjects were right-handed as determined by the Edinburgh Handedness Questionnaire [Oldfield, 1971].

From the data collected under the Sibling Study, we chose all available schizophrenic patients from whom we had good MEG resting recordings. For unaffected siblings, we had a few additional resting recordings available, but we chose the first 38 datasets to maintain a matched *n*-number with the patients. We needed to select 76 healthy control datasets from a large pool available to us, and we chose healthy control datasets that best matched the age and gender profile of the clinical datasets.

Main Comparison

Thirty-eight schizophrenic patients (11 females, 27 males; mean age: 31.2 ± 9.8, age range: 18.4–50.0) and 38 healthy controls (11 females, 27 males; mean age: 32.5 ± 10.8, age range: 20.0–54.2) were chosen as a matched sample from the sibling study.

Second Comparison

Thirty-eight unmedicated unaffected siblings of schizophrenic individuals (27 females, 11 males; mean age: 37.2 ± 11.3, age range: 18.9–54.7) and 38 healthy controls (27 females, 11 males; mean age: 36.5 ± 11.6, age range: 18.7–55.9) that did not overlap with the main comparison control group were chosen as a matched sample from the sibling study.

Procedure

Patients were seated in a lit, magnetically shielded room (MSR) composed of μ-metal and aluminum to reduce magnetic noise reaching the biomagnetometer. The chair was positioned at a fifteen degree angle from the vertical and instructions were delivered to subjects via an intercom system while subject behavior was monitored via a camera. Instructions were to rest with eyes closed until informed that the four-minute recording session was complete. The resting task analyzed in the current study was the first task within a battery of five MEG tasks in the sibling study agenda. The four additional tasks included a passive single-tone auditory task, an auditory oddball P300 paradigm, a gender discrimination task, and a working memory n-back condition.

Data Acquisition

MEG signals were continuously recorded using a SQUID sensor array consisting of 275 radial first-order gradiometers uniformly distributed over the inner surface of a whole-head helmet (the former CTF Systems, Coquitlam BC, Canada).

Real-time head position inside the magnetometer was determined by digitizing the position of reference coils that were attached to the nasion and bilateral preauricular points of each subject. The three fiducial points were also photographed for each participant as a means to coregister their MEG signals and their anatomical MRI (3T General Electric MRI scanner) data onto a common coordinate system.

Preprocessing

Raw neuromagnetic data was digitized at a sampling rate of 600 Hz with a bandwidth of 0–150 Hz and filtered in synthetic third gradient mode for online, background noise cancellation. Direct current (DC) offset removal was achieved using a minimal high-pass filter (0.61 Hz) and a powerline filter (60 Hz and higher harmonics).

The MEG signals were transformed into three-dimensional estimates of source power using synthetic aperture magnetometry (SAM) (Vrba and Robinson, 2001). Each voxel within the cortex is associated with a beamformer (275 × 1 vector), a unique set of weighting factors that SAM generates from the recorded magnetic field at each sensor, to generate a volumetric representation of brain activity. The filter output at each voxel is a virtual channel, a linear combination of the measurements over time for that specific brain location. SAM determines optimal spatial filters based on a minimum-variance beamformer that estimates current dipole power changes in a voxel within particular time windows and frequency bands. The optimal orientation of the dipole was estimated using the vector based approach of Sekihara et al (2001). A dipole spacing of 7.5 mm, corresponding to a cubic voxel width of 7.5 mm, was used for each dataset in this study.

We used single-state SAM imaging to estimate the power source distribution in the brain; normalization was accomplished via a constant noise estimate (i.e., Estimated Power = Raw Source Power/Constant Noise Estimate). A more detailed explanation of SAM power and constant noise estimations is included in the Appendix.

The initial and final 10 s of each dataset were excluded in the analysis. As such, the power of the SAM filter output at each virtual channel was accumulated across 220 s of the four-minute duration of the resting task.

The SAM covariance matrix was calculated in the traditional frequency bands seen in electrophysiological literature as follows: delta (0.9–4 Hz), theta (4–8 Hz), alpha (8–14 Hz), beta (14–30 Hz), gamma (30–80 Hz), and super-gamma (80–150 Hz).

Data Analysis

Talairach aligned volumes for each subject were computed to produce four 3D-mean maps (38 schizophrenic patients, 38 unaffected siblings, and two sets of 38 healthy controls) of brain activity via analysis of functional neural images (AFNI) software [Cox, 1996]. Additionally, 3D t-tests were computed for statistical purposes; they were used to determine whether any difference between healthy controls and patients or siblings was significant.

To account for the possibility of Type I errors, we used a false discovery rate multiple comparison test developed by Benjamini and Hochberg [Benjamini and Hochberg, 1995] via the AFNI program "3dFDR". Derived from the distribution of P-values in the dataset, the program generates a statistical threshold that predicts the false discovery rate among all significant voxels. We used a threshold of $q = 0.1$, which indicates a 10% false discovery rate, as suggested for neuroimaging studies [Genovese et al., 2001]. The "3dFDR" method also remains valid under conditions of high positive correlations in a dataset, which is often observed in neighboring SAM voxels [Nichols and Hayasaka, 2003].

RESULTS

3D t-tests ran between healthy controls from the main comparison and healthy controls from the second comparison showed no significant results.

TABLE I. Bandwidth versus false discovery rate for schizophrenic patients versus healthy controls

Bandwidth (Hz)	P-value	q-value
0.9–4	1.1×10^{-2}	0.93
4–8	6.6×10^{-3}	0.79
8–14	6.9×10^{-3}	1.00
14–30	5.9×10^{-3}	0.89
30–80	1.0×10^{-4}	0.08
80–150	8.0×10^{-4}	0.31

Main Comparison

Of the six 3D t-tests comparing healthy controls and patients across various frequency bands, the gamma bandwidth (30–80 Hz) was the only map that resulted in statistically significant voxels (Table I). Significant voxels contained a maximum q-value (false positive rate) of 0.1, which corresponded to a maximum P-value of 1.4×10^{-3}. The significant region of interest (ROI) consisted of 42 contiguous voxels (volume = 17,719 mm^3) in the posterior region of the medial parietal cortex (see Fig. 1). Specifically, the ROI overlapped with the bilateral precuneus (36.7%), cuneus (23.7%), PCC (2.5%), middle occipital gyrus (2.0%), and cingulate gyrus (1.0%). Healthy controls displayed higher SAM power averaged across the ROI voxels (9.19 ± 0.83) when compared with patients (8.04 ± 1.52).

We also wished to address whether the significance of the ROI encompassed only a subset of the gamma frequency band, or whether the significance was across the entire bandwidth. Furthermore, we sought to identify how the frequency of magnetic oscillations within the ROI differed between healthy controls and patients outside of the gamma bandwidth. To achieve these goals, we developed a sliding bandwidth window analysis.

Single-state SAM analysis was computed for 145 narrow bandwidth windows of 3.1 Hz. The overlapping bandwidths were shifted by 1.0 Hz for each SAM calculation, beginning with 2–5.1 Hz and ending with 146–149.1 Hz. The high frequency of the last bandwidth window (149.1 Hz) was just below the one-quarter sampling rate of 600 Hz (i.e., one-half of the Nyquist frequency). For each bandwidth window, 3D-mean maps for both healthy controls and patients were produced. This analytical approach allowed us to investigate the mean power in the gamma ROI (42 voxels) across narrow, overlapping frequency bands. It was intended to allow us to elucidate the differences in neuromagnetic activity in the ROI between healthy controls and schizophrenic patients across an entire spectrum of frequencies.

Using this approach, we found that healthy controls showed more SAM power than patients across gamma (30–80 Hz) and super-gamma (80–150 Hz) frequencies. However, across delta (0.9–4 Hz), theta (4–8 Hz), and alpha (8–14 Hz) frequencies, patients and healthy controls interchanged in demonstrating more SAM power (see Fig. 2). We also found that the significance (q < .05) of schizophrenic patients' decrease in gamma power in the ROI overlapped almost exclusively between 30 Hz and 70 Hz, with a few scattered significant bandwidths in higher frequencies (see Fig. 3).

Second Comparison

The gamma frequency band (30–80 Hz) was the only 3D-ttest map comparing healthy controls and unaffected siblings that resulted in statistically significant voxels (Table II). Significant voxels contained a maximum q-value (false positive rate) of 0.1, which corresponded to a maximum P-value of 5.6×10^{-3}. There were two significant ROIs in the gamma bandwidth. One ROI contained 44 con-
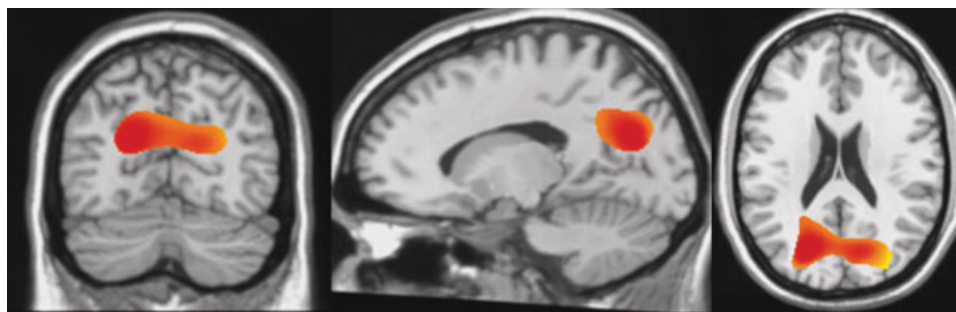

Figure 1.

From Left to Right: Axial (x = 86), Coronal (y = 65), Sagittal (z = 147) Significant voxels in the 3D-ttest comparing resting state conditions between healthy controls and schizophrenic patients in the gamma band (30–80 Hz) region. The significant ROI consists of 42 contiguous (there were no isolated) 7.5 mm width resolution voxels in the posterior region of the medial parietal lobule. Images were centered on the voxel representing the maximum intensity for the entire cluster (15, 67.5, 21.2). The majority of the cluster directly overlapped with bilateral precuneus (36.7%), cuneus (23.7%), PCC (2.5%), middle occipital gyrus (2.0%), and cingulate gyrus (1.0%). All other anatomical overlap accounted for less than 1.0% of the ROI as determined via the AFNI command "whereami bmask." For visualization, data were smoothed using a cubic spline.
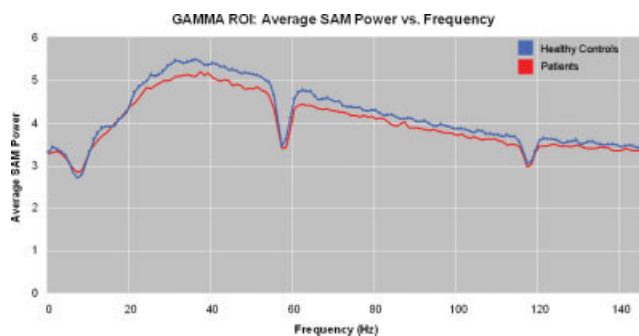
Figure 2.

SAM power averaged across the 42 significant voxels in the gamma ROI from the 3D-ttest comparing healthy controls and schizophrenic patients. Across gamma (30–80 Hz) and super-gamma (80–150 Hz) bandwidths, healthy controls showed more SAM power than patients. However, SAM power of patients and healthy controls toggled in the ROI across delta (0.9–4 Hz), theta (4–8 Hz), and alpha (8–14 Hz) bandwidths, and beta (14–30 Hz) bandwidths. The large dips in frequencies centered around 60 Hz and 120 Hz represent filtered powerline frequencies.

tiguous voxels (volume = 18,563 mm^3) in similar brain areas as the ROI from the main comparison, although lateralized to the left. The majority of the ROI overlapped with the middle occipital gyrus (38.5%), lingual gyrus (17.3%), cuneus (9.4%), inferior occipital gyrus (6.6%), fusiform gyrus (3.2%), inferior temporal gyrus (2.5%), and middle temporal gyrus (2.1%). Healthy controls displayed
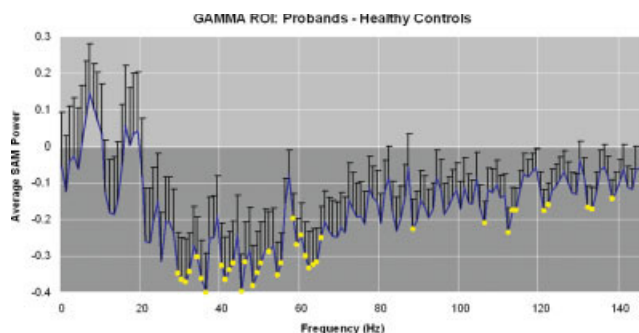

Figure 3.

The standard of error of the difference in the 42-voxel gamma ROI between healthy controls and schizophrenic patients is shown across a spectrum of frequencies. Yellow circles represent frequency windows with significant differences and the darkened background represents negative differences of the average SAM power (bandwidths in which healthy controls showed more SAM power than patients). The majority of significant bandwidth windows occurred between about 30 Hz and 70 Hz; however, scattered significant frequencies occurred in higher bandwidths as well. The interruption of significance-representing yellow circles in the spike around 60 Hz can be attributed to powerline filtration.

TABLE II. Bandwidth versus false discovery rate for unaffected siblings versus healthy controls

Bandwidth (Hz)	P-value	q-value
0.9–4	1.8×10^{-3}	0.66
4–8	8.3×10^{-3}	0.83
8–14	2.4×10^{-4}	0.74
14–30	2.3×10^{-4}	0.41
30–80	5.6×10^{-5}	0.09
80–150	2.7×10^{-4}	0.24

higher SAM power across the ROI (5.17 ± 0.84) when compared with unaffected siblings (4.42 ± 0.78). Another ROI contained 123 contiguous voxels (volume = 51,894 mm^3) that overlapped with the superior frontal gyrus (48.2%), middle frontal gyrus (22.7%), medial frontal gryus (8.9%), and precentral gyrus (7.4%). Unaffected siblings displayed higher SAM power averaged across the ROI voxels (7.06 ± 1.76) when compared with healthy controls (6.22 ± 1.68).

We used the same sliding bandwidth analysis discussed above to investigate the neuromagnetic activity across an entire range of frequencies for the 44-voxel unaffected siblings ROI that contained similar brain regions as the 42-voxel patient ROI. We found that healthy controls showed more SAM power than unaffected siblings across all frequencies (2–149.1 Hz) (see Fig. 4). Unlike the patient sliding bandwidth analysis, none of the individual bandwidth windows of 3.1 Hz showed significance.

Post Hoc Gamma 3D-Mean Analysis

We wished to investigate whether, within the gamma bandwidth, default network brain regions were significantly more activated than other brain areas. As such, we
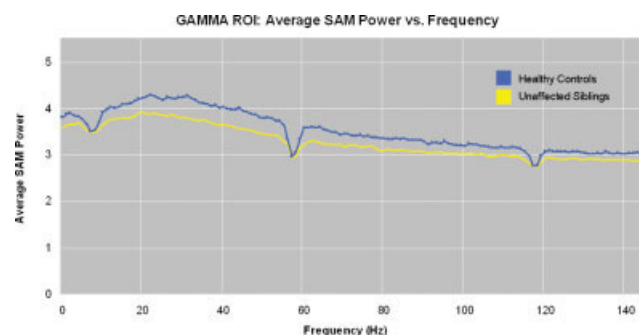

Figure 4.

SAM power averaged across the 44 significant voxels in the gamma ROI from the 3D-ttest comparing healthy controls and unaffected siblings of schizophrenic patients. Healthy controls had more SAM power than unaffected siblings across all bandwidth windows (between 2 Hz and 149.1 Hz), although none of the individual bandwidths were significant. The large dips in frequencies centered around 60 Hz and 120 Hz represent filtered powerline frequencies.

TABLE III. Top 100 SAM power voxels in 3D-mean gamma map of healthy controls from the main comparison

Atlas region	Bilateral	Left	Right
Precuneus	37	24	13
Precentral gyrus	18.5	9	9.5
Inferior parietal gyrus	14	12	2
Cingulate gyrus	13	9	4
Paracentral gryus	8	4	4
Postcentral gyrus	7.5	3	4.5
Middle frontal gyrus	1	0	1
Medial frontal gyrus	1	0	1
	100	61	39

TABLE V. Top 100 SAM power voxels in 3D-mean gamma map of healthy controls from the second comparison

Atlas region	Bilateral	Left	Right
Precuneus	38	23	15
Cingulate gyrus	18	12	6
Postcentral gyrus	14	8	6
Inferior parietal gyrus	11.5	7	4.5
Precentral gryus	9	6	3
Paracentral gyrus	8.5	6	2.5
Middle frontal gyrus	1	0	1
	100	62	38

analyzed the gamma 3D-mean map for each group (patients, unaffected siblings, and healthy controls in both comparisons) to determine whether default brain areas were the most active regions within the brain. Specifically, for each dataset, we located, via the "whereami" function in AFNI, the 100 voxels with the highest SAM power and determined the brain region closest to each voxel as defined by the Talairach-Tournoux Atlas System.

We discovered that, for all subject groups, the 100 voxels demonstrating the most SAM power coincided with several resting brain areas (Tables III–VI). The top six areas of SAM activity in all subject groups included the precuneus, cingulate gyrus, postcentral gyrus, inferior parietal gyrus, paracentral gyrus, and precentral gyrus. The middle frontal gyrus and medial frontal gyrus were the only other brain regions within the top 100 voxels. These two regions demonstrated the most activity in the patients map (Table IV), but only accounted for 6.5% of voxels. The precuneus displayed the highest number of voxels for all four groups; healthy controls in the second comparison (38%, Table V), healthy controls in the main comparison (37%, Table III), unaffected siblings (28%, Table VI), and patients (22%, Table IV).

Relative Risk Analysis

A relative risk analysis was performed to determine whether the observed reduction of resting gamma power

TABLE IV. Top 100 SAM power voxels in 3D-mean gamma map of schizophrenic patients

Atlas region	Bilateral	Left	Right
Precuneus	22	12	10
Precentral gyrus	20	12.5	7.5
Postcentral gyrus	14	8	6
Cingulate gyrus	14	6	8
Paracentral gryus	13	8	5
Inferior parietal gyrus	10.5	5.5	5
Medial frontal gyrus	5	3	2
Middle frontal gyrus	1.5	0	1.5
	100	55	45

in unaffected siblings may represent an intermediate phenotype due to genetic risk factors. The power in the gamma band for the ROI from the patients described above was calculated as an individual measure for all subjects. Averages for each group were as follows: healthy controls in the main comparison (9.19 ± 0.83), healthy controls in the second comparison (9.18 ± 0.97), unaffected siblings (8.99 ± 1.25), and schizophrenic patients (8.04 ± 1.52). As expected from the 3D-mean analysis, the mean difference should be highly significant: the schizophrenic patient group showed a significant reduction compared to the healthy control group in the main comparison (t-value: $5.33 \times 10–5$; P-value: <0.00001) (we only report this statistic to confirm the main finding described above; we selected the same 42 significant voxels from the original patient ROI) and the unaffected siblings group did not. However, using a cutoff of two standard deviations below the mean, there were six individuals in the unaffected siblings group when compared with one in the healthy control group for an odds ratio of 6:1.

DISCUSSION

Our results are consistent with our hypothesis that schizophrenic patients may show less baseline activity in the MEG gamma band region. Aberrant baseline activity in schizophrenic patients has now been observed in both slow-frequency fluctuations of BOLD signals and here in the gamma frequencies of MEG signals [Bluhm et al., 2007;

TABLE VI. Top 100 SAM power voxels in 3D-mean gamma map of unaffected siblings

Atlas region	Bilateral	Left	Right
Precuneus	28	14	14
Cingulate gyrus	21	11	10
Precentral gyrus	19.5	9	10.5
Postcentral gryus	16.5	5.5	11
Inferior parietal gyrus	10.5	3.5	7
Paracentral gyrus	3.5	3.5	0
Middle frontal gyrus	1	0	1
	100	46.5	53.5

Garrity et al., 2007; Liang et al., 2006; Liu et al., 2008; Zhou et al., 2007a,b]. Our current observations may serve to support the conjecture that slow frequency (<0.1 Hz) fluctuations in the BOLD signal may be associated with electrophysiological gamma power.

Although we did not find beta band differences in our analysis, previous studies using the SAM source localization technique have correlated event-related desynchronization (ERD) of MEG waves in 5–10 Hz (high theta/low alpha) and 15–25 Hz (beta) with cortical hemodynamic fMRI response [Singh et al., 2002]. However, these studies have all used cognitive paradigms that were not collected at rest, and that may account for the distinction of our current gamma band results.

Although Garrity et al. [Garrity et al., 2007] observed laterality differences in the reduction of schizophrenic resting brain activity, the current study found bilateral reduction of resting activity in patients. Limitation of our study in terms of sensitivity to lateralized sources may account for these differences. However, controversy remains as to whether patients with schizophrenia show a reversal or reduction of lateralization [Dragovic et al., 2005].

Importantly, the precuneus appears to show the most resting state gamma SAM power for healthy control groups (Tables III and V), patients (Table IV), and unaffected siblings (Table VI). An average of these four subject groups shows that the precuneus accounted for 31.25% of the 100 voxels with the highest SAM gamma power. Our results are consistent with resting state PET studies in which the precuneus demonstrated the highest metabolic rate in healthy individuals, consuming 35% more glucose than any other cerebral cortex region [Gusnard and Raichle, 2001]. Such consistency across diverse neuroimaging methods suggests that this area of the brain in the posteromedial portion of the parietal lobe warrants more investigation than it has traditionally received.

Until recently, in fact, the precuneus has elicited little interest. One possibility is that its anatomical setting, hidden in the interhemispheric fissure and enclosed by the sagittal sinus and bridging veins, made it a challenging location to study before the advent of advanced neuroimaging techniques [Cavanna and Trimble, 2006]. Along these lines, the precuneus is rarely lesioned in strokes or accidents [Cavanna and Trimble, 2006]. However, its widespread connections suggest that it is an important association area that performs a wide spectrum of higher-order functions. In particular, the precuneus comprises a larger fraction of brain volume in humans than in other primates and animals, is among the last areas to myelinate, and contains the most complex columnar cortical configuration in the human brain [Cavanna and Trimble, 2006]. In all, anatomical and connectivity data implicate that the precuneus is likely to be engaged in advanced mental functions.

A recent review article on the precuneus in hemodynamic neuroimaging studies of healthy humans by Cavanna and Trimble [Cavanna and Trimble, 2006] suggests that this brain area may have a central role in a broad array of cognitive functions including visuospatial imagery, episodic memory retrieval, and internal versus external awareness. Importantly, aberrancy of these brain areas in schizophrenia, as evidenced by consistently low scores in visuospatial tasks [Fleming et al., 1997; Keefe et al., 1997; Park and Holzman, 1992; Weickert et al., 2000], episodic memory retrieval tasks [Danion et al., 1999; Kuperberg and Heckers, 2000; Tendolkar et al., 2002], and reduced ability to differentiate external versus internal stimuli [Allen et al., 2004; Frith, 1995] may be relevant to our findings of decreased baseline activity in these brain regions during rest.

Anatomical imaging has also offered strong evidence that schizophrenic individuals may have structural differences in the precuneus. For instance, anatomical MRI studies have discovered precuneus gray matter thinning in schizophrenic patients [Hulshoff et al., 2001], and this reduction in volume does not appear to be significantly different between patients who are on and off medications [Narr et al., 2005]. Also, directly supporting the findings of our current study, Mitelman et al. [Mitelman et al., 2004] concluded that their discovery of reduced cortical thickness in the PCC of schizophrenic patients is consistent with reduced modulation of these regions "especially during unstructured periods such as rest."

Our study addressed the three questions outlined in the introduction. First, we found that resting SAM analysis of MEG data resulted in a network of brain regions that overlapped with the so-called "default network" seen in other neuroimaging techniques, in particular the precuneus. Second, the highest SAM power occurred primarily in the precuneus in the gamma frequency band for all subject groups. Third, this gamma baseline activity appears to be significantly reduced in schizophrenic patients and their unaffected siblings. Furthermore, the results of the present study add to the growing evidence (by means of structural imaging, functional imaging, and neuropsychological testing) that the brain regions involved in resting networks may be abnormal in schizophrenia.

The current study also provides compelling, albeit preliminary, evidence that baseline activity may be a potential avenue for future schizophrenic research. Resting state analysis has already appeared to elicit meaningful results in other clinical populations, particularly Alzheimer's disease [Eustache et al., 2004; Greicius et al., 2004; Johnson et al., 1998; Minoshima et al., 1997; Rombouts et al., 2005], and has led some authors to believe that such methods may one day be used for preclinical prediction of the disorder [Johnson et al., 1998]. Additionally, designs using the resting state method have the added benefit that they do not rely extensively on behavioral analysis in comparison to conventional cognitive designs [Esposito et al., 2006].

Resting state designs are beginning to receive more notice in neuroimaging research, and are also beginning to elicit promising evidence that baseline activity may not simply reflect an irrelevant response to being positioned in the scanner, as some have argued [Morcom and Fletcher, 2006]. Fox et al. [Fox et al., 2005], for example, contends

that this is not the case because their fMRI study found that resting state conditions are duplicated across different states including eyes closed, eyes open with visual fixation, and eyes opened without visual fixation. The authors argue that the reproducibility of their findings demonstrates that baseline activity cannot be attributed to the artifice of low-level tasks like fixation, presence or absence of visual input, or eye movements.

Another potential argument against resting state designs for clinical populations is that patients may experience more anxiety in the artificial environment of the scanner, making it difficult to reach a self-reflective state and accounting for the reported anomalies in the default network regions. Bluhm et al. [Bluhm et al., 2007] thinks this is unlikely, however, because anxious subjects exhibit comparable activity levels in the default mode regions with nonanxious subjects [Simpson et al., 2001]. For schizophrenic populations, moreover, another obvious dispute is whether the deficit can be explained by antipsychotic medication. Our current finding that unaffected siblings of patients display a similar significant reduction of gamma resting activity and show an odds ratio of 6:1 across the patient ROI suggests that the reduction seen in the baseline activity of schizophrenic patients may not be due to medication alone.

One limitation of the current study is that the resting task was originally designed to acquaint participants with the MEG setting prior to the collection of four additional tasks. Unfortunately, this setup does not serve to lessen the artificiality of the scanning environment during the resting task, and the data may reflect more of how different populations experience the MEG setting, as opposed to how "default mode" activity varies across different populations. In other words, it is difficult to verify that the decreased resting gamma power observed in patients is a result of pathological biology, rather than abnormal behavior. An additional limitation of our study is that not each unaffected sibling was directly matched with his or her schizophrenic family member. Perhaps an analysis in which patients and unaffected siblings are paired by family may result with unaffected siblings acting more as an intermediate phenotype to support the notion that the observed reduction of resting gamma activity in patients is partially the result of genetics and not antipsychotic medications alone. What is more, we were not able to examine a set of unmedicated patients; this is something that, if achieved in the future, may provide insight concerning the degree that patients' gamma resting activity is modulated by medications. Regardless of its limitations, the current study produces meaningful results that suggest that resting conditions may not serve as adequate control conditions in neuroimaging task designs when clinical populations show significant differences in their resting brain activity.

In subsequent studies that desire to address the question of default mode activity, it would be appropriate to administer a debriefing with each participant after their scan and assess their level of anxiety while in the scanner. Future studies on schizophrenia resting activity may also attempt to explore the subtypes of the illness [Malaspina et al., 2004] as well as correlate clinical variables in relation to individual resting activity. It may also be of interest for additional MEG resting studies to investigate the temporal dynamics of gamma band SAM power, as the current study examined gamma band power accumulated across 220 s.

ACKNOWLEDGMENTS

REFERENCES

Allen PP, Johns LC, Fu CHY, Broome MR, Vythelingum GN, McGuire PK (2004): Misattribution of external speech in patients with hallucinations and delusions. Schizophr Res 69:277–287.

Benjamini Y, Hochberg Y (1995): Controlling the false discovery rate: A practical and powerful approach to multiple testing. J Roy Stat Soc 57:289–300.

Bluhm RL, Miller J, Lanius RA, Osuch EA, Boksman K, Neufeld RWJ, Theberge J, Schaefer B, Williamson P (2007): Spontaneous low-frequency fluctuations in the bold signal in schizophrenic patients: Anomalies in the default network. Schizophr Bull 33:1004–1012.

Bosboom JL, Stoffers D, Stam CJ, van Dijk BW, Verbunt J, Berendse HW, Wolters ECH (2006): Resting state oscillatory brain dynamics in Parkinson's disease: An MEG study. Clin Neurophys 117:2521–2531.

Bruns A, Eckhorn R, Jokeit H, Ebner A (2000): Amplitude envelope correlation detects coupling among incoherent brain signals. Neuroreport 11:1509–1514.

Buzsaki G, Draguhn A (2004): Neuronal oscillations in cortical networks. Science 304:1926–1929.

Callicott JH, Egan MF, Bertolino A, Mattay VS, Langheim FJP, Frank JA, Weinberger DR (1998): Hippocampal N-acetyl aspartate in unaffected siblings of patients with schizophrenia: A possible intermediate neurobiological phenotype. Biol Psychiatry 44:941–950.

Cavanna AE, Trimble MR (2006): The precuneus: A review of its functional anatomy and behavioural correlates. Brain 129:564–583.

Cox RW (1996): AFNI: Software for analysis and visualization of functional magnetic resonance neuroimages. Comput Biomed Res 29:162–173.

Danion JM, Rizzo L, Bruant A (1999): Functional mechanisms underlying impaired recognition memory and conscious awareness in patients with schizophrenia. Arch Gen Psychiatry 56:639–644.

Dragovic M, Hammond G, Badcock JC, Jablensky A (2005): Laterality phenotypes in patients with schizophrenia, their siblings and controls: Associations with clinical and cognitive variables. Br J Psychiatry 187:221–228.

Egan MF, Goldberg TE, Gscheidle T, Weirich M, Bigelow LB, Weinberger DR (2000): Relative risk of attention deficits in siblings of patients with schizophrenia. Am J Psychiatry 157:1309–1316.

Esposito F, Bertolino A, Scarabino T, Latorre V, Blasi G, Popolizio T, Tedeschi G, Cirillo S, Goebel R, Di Salle F (2006):

Independent component model of the default-mode brain function: assessing the impact of active thinking. Brain Res Bull 70:263–269.

Eustache F, Piolino P, Giffard B, Viader F, De La Sayette V, Baron J, Desgranges B (2004): 'In the course of time': A PET study of the cerebral substrates of autobiographical amnesia in Alzheimer's disease. Brain 127:1549–1560.

Fleming K, Goldberg TE, Binks S, Randolph C, Gold JM, Weinberger DR (1997): Visuospatial working memory in patients with schizophrenia. Biol Psychiatry 41:43–49.

Fox MD, Snyder AZ, Vincent JL, Corbetta M, Van Essen DC, Raichle ME (2005): The human brain is intrinsically organized into dynamic, anticorrelated functional networks. Proc Natl Acad Sci USA 102:9673–9678.

Frith C (1995): Functional imaging and cognitive abnormalities. Lancet 346:615–620.

Garrity AG, Pearlson GD, McKiernan K, Lloyd D, Kiehl KA, Calhoun VD (2007): Aberrant "default mode" functional connectivity of schizophrenia. Am J Psychiatry 164:450–457.

Genovese CR, Lazar NA, Nichols T (2001): Thresholding of statistical maps in functional neuroimaging using the false discovery rate. Neuroimage 15:870–878.

Georgopoulos AP, Karageorgiou E, Leuthold AC, Lewis SM, Lynch JK, Alonso AA, Aslam Z, Carpenter AF, Georgopoulos A, Hemmy LS, Koutlas IG, Langheim FJP, McCarten JP, McPherson SE, Pardo JV, Pardo PJ, Parry GJ, Rottunda SJ, Segal BM, Sponheim SR, Stanwyck JJ, Stephane M, Westermeyer JJ (2007): Synchronous neural interactions assessed by magnetoencephalography: A functional biomarker for brain disorders. J Neural Eng 4:349–355.

Goldberg TE, David A, Gold JM (2003): Neurocognitive deficits in schizophrenia. In: Hirsch SR, Weinberger DR, editors. Schizophrenia. Oxford: Blackwell Publishing. pp 168–184.

Greicius MD, Menon V (2004): Default-mode activity during a passive sensory task: Uncoupled from deactivation but impacting activation. J Cogn Neurosci 16:1484–1492.

Greicius MD, Krasnow B, Reiss AL, Menon V (2003): Functional connectivity in the resting brain: A network analysis of the default mode hypothesis. Proc Natl Acad Sci USA 100:253–258.

Greicius MD, Srivastava G, Reiss AL, Menon V (2004): Default-mode network activity distinguishes Alzheimer's disease from healthy aging: Evidence from functional MRI. Proc Natl Acad Sci USA 101:4637–4642.

Gusnard DA, Raichle ME (2001): Searching for a baseline: Functional imaging and the resting human brain. Nat Rev Neurosci 2:685–694.

Gusnard DA, Akbudak E, Shulman GL, Raichle ME (2001): Medial prefrontal cortex and self-referential mental activity: Relation to a default mode of brain function. Proc Natl Acad Sci USA 98:4259–4264.

Harrison BJ, Yucel M, Pujol J, Pantelis C (2007): Task-induced deactivation of midline cortical regions in schizophrenia assessed with fMRI. Schizophr Res 91:82–86.

Hulshoff HE, Schnack HG, Mandl RCW, van Haren NEM, Koning H, Collins L, Evans AC, Kahn RS (2001): Focal gray matter density changes in schizophrenia. Arch Gen Psychiatry 58:1118–1125.

Johnson KA, Jones K, Holman BL, Becker JA, Spiers PA, Satlin A, Albert MS (1998): Preclinical prediction of Alzheimer's disease using SPECT. Neurology 50:1563–1572.

Keefe RSE, Lees-Roitman SE, Dupre RL (1997): Performance of patients with schizophrenia on a pen and paper visuospatial working memory task with short delay. Schizophr Res 26:9–14.

Kuperberg G, Heckers S (2000): Schizophrenia and cognitive function. Curr Opin Neurobiol 10:205–210.

Laufs H, Krakow K, Sterzer P, Eger E, Beyerle A, Salek-Haddadi A, Kleinschmidt A (2003): Electroencephalographic signatures of attentional and cognitive default modes in spontaneous brain activity fluctuations at rest. Proc Natl Acad Sci USA 100:11053–11058.

Lawrence NS, Ross TJ, Hoffmann R (2003): Multiple neuronal networks mediate sustained attention. J Cogn Neurosci 15:1028–1038.

Liang M, Zhou Y, Jiang T, Liu Z, Tian L, Liu H, Hao Y (2006): Widespread functional disconnectivity in schizophrenia with resting-state functional magnetic resonance imaging. Neuroreport 17:209–213.

Liu Y, Liang M, Zhou Y, He Y, Hao Y, Song M, Yu C, Liu H, Liu Z, Jiang T (2008): Disrupted small-world networks in schizophrenia. Brain 131:945–961.

Malaspina D, Harkavy-Friedman J, Corcoran C, Mujica-Parodi L, Printz D, Gorman JM, Heertum RV (2004): Resting neural activity distinguishes subgroups of schizophrenia patients. Biol Psychiatry 56:931–937.

Mazoyer B, Zago L, Mellet E, Bricogne S, Etard O, Houde O, Crivello F, Joliot M, Petit L, Tzourion-Mazoyer N (2001): Cortical networks for working memory and executive functions sustain the conscious resting state in man. Brain Res Bull 54:287–298.

McKiernan KA, Kaufman JN, Kucera-Thompson J, Binder JR (2003): A parametric manipulation of factors affecting task-induced deactivation in functional neuroimaging. J Cogn Neurosci 15:394–408.

Minoshima S, Giordani B, Berent S, Frey KA, Foster NL, Kuhl DE (1997): Metabolic reduction in the posterior cingulate cortex in very early Alzheimer's disease. Ann Neurol 42:85–94.

Mitelman SA, Shihabuddin L, Brickman AM, Hazlett EA, Buchsbaum MS (2004): Volume of the cingulate and outcome in schizophrenia. Schizophr Res 72:91–108.

Morcom AM, Fletcher PC (2006): Does the brain have a baseline? Why we should be resisting a rest. Neuroimage 37:1073–1082.

Narr KL, Toga AW, Szeszko P, Thompson PM, Woods RP, Robinson D, Sevy S, Wang Y, Schrock K, Bilder RM (2005): Cortical thinning in cingulate and occipital cortices in first episode schizophrenia. Biol Psychiatry 58:32–40.

Nichols T, Hayasaka S (2003): Controlling the familywise error rate in functional neuroimaging: A comparative review. Stat Methods Med Res 12:419–446.

Oldfield RC (1971): The assessment and analysis of handedness: The Edinburgh handedness inventory. Neuropsychologia 9:97–113.

Park S, Holzman PS (1992): Schizophrenics show spatial working memory deficits. Arch Gen Psychiatry 49:975–982.

Raichle ME, MacLeod AM, Snyder AZ, Powers WJ, Gusnard DA, Shulman GL (2001): A default mode of brain function. Proc Natl Acad Sci USA 98:676–672.

Rombouts SARB, Barkhof F, Goekoop R, Stam CJ, Scheltens P (2005): Altered resting state networks in mild cognitive impairment and mild Alzheimer's disease: An fMRI study. Hum Brain Mapp 26:231–239.

Sekihara K, Nagarajan SS, Poeppel D, Marantz A, Miyashita Y (2001): Reconstructing spatio-temporal activities of neural sources using an MEG vector beamformer technique. IEEE Trans Biomed Eng 48:760–771.

Shulman GL, Fiez JA, Corbetta M, Buckner RL, Miezin FM, Raichle ME, Petersen SE (1997): Common blood flow changes across visual tasks: II. Decreases in cerebral cortex. J Cogn Neurosci 9:648–663.

Simpson JR Jr, Drevets WC, Snyder AZ, Gusnard DA, Raichle ME (2001): Emotion-induced changes in human medial prefrontal cortex: II. During anticipatory anxiety. Neurobiology 98:688–693.

Singh KD, Barnes GR, Hillebrand A, Forde EME, Williams AL (2002): Task-related changes in cortical synchronization are spatially coincident with the hemodynamic response. Neuroimage 16:103–114.

Stam CJ, Jones BF, Manshanden I, van Cappellen van Walsum AM, Montez T, Verbunt JP, de Munck JC, van Dijk BW, Berendsea HW, Scheltens P (2006): Magnetoencephalographic evaluation of resting-state functional connectivity in Alzheimer's disease. Neuroimage 32:1335–1344.

Tendolkar I, Ruhrmann S, Brockhaus A, Pukrop R, Klosterkotter J (2002): Remembering or knowing: Electrophysiological evidence for an episodic memory deficit in schizophrenia. Psychol Med 32:1261–1271.

Vrba J, Robinson SE (2001): Signal processing in magnetoencephalography. Methods 25:249–271.

Weickert TW, Goldberg TE, Gold JM, Bigelow LB, Egan MF, Weinberger DR (2000): Cognitive impairments in patients with schizophrenia displaying preserved and compromised intellect. Arc Gen Psychiatry 57:907–913.

Weissman DH, Roberts KC, Visscher KM, Woldorff MG (2006): The neural bases of momentary lapses in attention. Nat Neurosci 9:971–978.

Winterer G, Egan MF, Raedler T, Sanchez C, Jones DW, Coppola R, Weinberger DR (2003): P300 and genetic risk for schizophrenia. Arch Gen Psychiatry 60:1158–1167.

Zhou Y, Liang M, Jiang T, Tian L, Liu Y, Liu Z, Liu H, Kuang F (2007a) Functional dysconnectivity of the dorsolateral prefrontal cortex in first-episode schizophrenia using resting-state fMRI. Neurosci Lett 417:297–302.

Zhou Y, Liang M, Tian L, Wang K, Hao Y, Liu H, Liu Z, Jiang T (2007b) Functional disintegration in paranoid schizophrenia using resting-state fMRI. Schizophr Res 97:194–205.

APPENDIX

For a given time window, filtered MEG data can be represented by the matrix X in which the rows contain data points for N sensor channels and the columns contain sensor values for all time points in the time window. The estimated magnetic activity that reached each sensor and originated from the source dipole was estimated using the forward solution, G_θ, an $N \times 1$ column vector. The theoretical forward model takes into account the orientation and location of the dipole. The optimal orientation of the dipole source, θ, was determined using the eigenvector based approach of Sekihara et al. [Sekihara et al., 2001].

Each voxel within the cortex is associated with a unique beamformer, H_θ, an $N \times 1$ vector set of weighting factors that SAM generates from both the recorded magnetic field at each sensor and the forward solution to generate a volumetric representation of brain activity. The filter output at each voxel is a virtual channel, $H_\theta^T X$, a linear combination of the measurements over time for that specific brain location.

The $N \times N$ covariance matrix C represents the covariance between sensor channels in the data matrix X after the mean of each channel has been removed. The ultimate goal of the spatial filtering technique is to determine an optimal beamformer that suppresses leakage (sensor noise, magnetic activity from extraneous brain sources, and environmental magnetic interference) while preserving the source strength of the dipole. This is achieved by minimizing $H_\theta^T C H_\theta$ under the constraint that $G_\theta^T H_\theta = 1$, in which the output, after applying the method of Lagrange multipliers, is known to be:

$$H_\theta = \frac{C^{-1} G_\theta}{G_\theta^T C^{-1} G_\theta} \tag{1}$$

The source power estimation in matrix notation can then be expressed as

$$\begin{aligned}
\hat{S}_\theta^2 \approx \left(H_\theta^T X\right)^2 &= \left(H_\theta^T X\right)\left(H_\theta^T X\right)^T \\
&= \left(H_\theta^T X\right)\left(H_\theta X^T\right) \\
&= H_\theta^T \left(X X^T\right) H_\theta \\
&= H_\theta^T C H_\theta
\end{aligned} \tag{2}$$

We used single-state pseudo Z-deviate SAM spatial filtering to estimate the power source distribution in the brain. The source power distribution described above produces low signal-to-noise ratios near the center of the head, where the source location is the most distant from the sensors. To compensate for the noise, normalization was accomplished via a constant noise estimate. The smallest eigenvalue from the covariance matrix was defined as the noise variance, v^2. An array Σ of N sensors with the constant noise variance was considered:

$$\Sigma = \begin{bmatrix} v_1^2 & \cdots & \cdots & 0 \\ \vdots & v_2^2 & \cdots & \vdots \\ \vdots & \vdots & \ddots & \vdots \\ 0 & \cdots & \cdots & v_N^2 \end{bmatrix} \tag{3}$$

The voxel's estimated sensor noise, $\hat{v}_\theta^2$, was calculated using the previously derived beamformer and the array of constant noise variance:

$$\hat{v}_\theta^2 = H_\theta^T \Sigma H_\theta \tag{4}$$

The normalized estimated power in the voxel then becomes a ratio of the estimated source power and the estimated noise variance of the voxel:

$$Z_\theta^2 = \frac{\hat{S}_\theta^2}{\hat{v}_\theta^2} = \frac{H_\theta^T C H_\theta}{H_\theta^T \Sigma H_\theta} \tag{5}$$